芸術科学会論文誌 Vol. 13, No. 1, pp. 21-33

An Estimation of Earthenware's Surface Shape Using Quadric Surfaces

Tsutomu Kinoshita[1] (Member) **Katsutsugu Matsuyama**[2] (Member)

Kouichi Konno[2] (Member)

1) Lattice Technology Co.,Ltd.

2) Graduate school of Engineering, Iwate Univ.

pxw05066@nifty.com, kmatsu@iwate-u.ac.jp, konno@eecs.iwate-u.ac.jp

Abstract

In most cases, earthenware is broken when it is excavated from ruins. This situation requires restoration for assembling the earthenware's pieces. The point clouds measured by a three-dimensional device are useful to restore the earthenware. Some methods to find adjacent pieces of earthenware using a computer have been proposed. These methods aim to restore broken earthenware by connecting adjacent pieces with using digital data. If, however, earthenware with large missing portions is restored, it is impossible to estimate the adjacent piece using local adjacency. Due to this, it is necessary to estimate the whole shape of earthenware. It is also possible to continue sequential local estimation for estimating whole shape of earthenware, but the distortion occurs in many cases. In this paper, we propose a method to estimate the whole shape of earthenware with quadric surfaces. Since most earthenware is produced to be as close as rotational shapes, quadric surfaces are suitable to represent rotational shapes. In our method, the uneven pattern on the surface is removed in the first step according to the Taubin's smoothing method. Next, the point cloud from which uneven patterns are removed is divided into several groups. After that, each point cloud is fitted to quadric surfaces represented by the algebraic equation. Finally, the sequences of points generated from quadric surfaces are interpolated and the free-form surfaces corresponding to the surface of the earthenware are generated.

1. Introduction

In most cases, earthenware is broken when it is excavated from ruins. Generally, all processes from classification of earthenware to assembly and restoration are done manually. Therefore, it takes much time to restore a large number of pieces of broken earthenware. The restoration also requires technical knowledge and experience and restoration work of a relic becomes heavy burden in the archaeological field. Moreover, manual restoration raises the risk for damaging earthenware pieces. In recent years the researches have been carried out to support earthenware restoration work by measuring earthenware with a three-dimensional measurement device and connecting earthenware pieces by using measured data [1-11].

Restoration of earthenware is classified into two types: one is to restore actual earthenware and the other is to create replicas. If earthenware is so precious to be designated as important cultural properties and if their replicas are created, it will be possible to exhibit them at different exhibition halls at same time. When replicas are created, it is also necessary to interpolate missing portions as much as possible to restore the correct condition of earthenware.

For interpolating missing portions of earthenware using the measurement data, a method to extract the portions from the peripheral shapes has been proposed [12]. In [12], however, it is difficult to restore missing portions because the shape and size of the missing portions have some restriction. In addition, if surfaces for the missing portions are generated from the peripheral surfaces, the whole shape might get distorted.

In this paper, we present a method to estimate earthenware's surface shape even if the surface data is incomplete. In our method, the point cloud is measured by a three-dimensional measurement device. After uneven patterns are removed from the point cloud [13], it is approximated for a quadric surface and the center axis of the surface is extracted. After that, to generate precise surfaces, the point cloud is divided into several groups according to the center axis. Then, each group is fitted to a suitable quadric surface. Finally, a free-form curve mesh is created from quadric surfaces and a free-form surface mesh is created from the free-form curve mesh. Thus, the complete

earthenware surface is represented by free-form surfaces. As a result of evaluating the distance between the measurement point cloud and the generated free-form surface, good results were obtained. Since all parts of the shape are defined as quadric surfaces, the shape is not distorted, and the normal vectors or cutting faces of any part of the earthenware surfaces can be easily obtained. Such information can be used not only for reproduction of the shape but for analyses upon creation of measured diagrams of earthenware.

2. Related Works

2.1 Removal of uneven portions

If a surface is generated from the polygon created from the point clouds of earthenware without processing the point cloud data, the quality of the generated curved surface becomes low, because uneven patterns remain. Due to this, the uneven pattern is regarded as noise of earthenware and our proposed method performs the smoothing process to remove the uneven pattern. Generally, the method of low-pass filter smoothing is used for this processing. This paper, however, uses the Taubin's method to create a smooth spherical shape since the Taubin's method based on the Laplace transform formula [13] can be executed in a short time.

2.2 Quadric form and ellipse fitting

As the method of fitting a quadric form to a point cloud, Fitzgibbon et al. [14] presented the method to fit an ellipse to two-dimensional point sequence. To be more specific, a quadric form is represented by a two-dimensional curve that minimizes the distance between the point sequence and the curve by using the Lagrange multiplier method. This method is solved by applying the elliptical constraint to the Lagrange multiplier method. Unfortunately, the purpose of Fitzgibbon et al. [14] is to approximate all points by a single ellipse. If the Fitzgibbon's method is applied to our method, complex shapes such as earthenware must be represented with one quadric surface. Due to this, we judged that it is difficult to apply the Fitzgibbon's method directly to three-dimensional pieces of earthenware.

2.3 Quadric surface fitting to point cloud

Douros presented the method [15], which extends the method of Fitzgibbon et al [14] to three-dimension and fits quadric surfaces to three-dimensional point clouds. The Douros' method defines the quadric form as a general one, and in the same manner as of the Fitzgibbon's method, point clouds are fitted to a quadric surface locally by using the Lagrange multiplier method. To be more specific, a quadric surface is fitted to a portion of a point cloud. The Douros' method projects points onto a quadric surface and calculates the curvature of the projection position as the curvature of the point. The Douros' method does not mention how to use curvature. He plans to use curvature in order to drive a 3D matching algorithm. The Douros' method generates a lot of small quadric surfaces and does not consider the continuity of surfaces. Moreover, his method cannot handle the shape that has missing parts because it is not necessary to know elements except curvature. Therefore, his method cannot be applied directly for fitting surfaces from the earthenware whose portions are missing.

2.4 Classification of surfaces

Only a few CAD software applications can support all kinds of quadric surfaces as the shape representation. Due to this, quadric surfaces may be approximated by free-form ones when the quadric surface appear. When quadric surfaces are converted to free-form ones, several processing are required: quadric surface division, creation of four-sided regions, or acquisition of tangent vectors or normal vectors. These processing are required to be divided depending on the type of quadric surfaces. In order to classify quadric surfaces, it is necessary to convert the form of Equation (1) of a quadric surface represented by a general quadric to the standard quadric form such as the one shown in Table 1. As the conversion method, principal-axis transformation described in section 2.5 is introduced.

$$
\begin{aligned}
&F(X,A) = AX = ax^2 + by^2 + cz^2 \\
&+ pxy + qyz + rzx \\
&+ ux + vy + wz + d = 0 \\
&A = \begin{bmatrix} a & b & c & p & q & r & u & v & w & d \end{bmatrix}^T \\
&X = \begin{bmatrix} x^2 & y^2 & z^2 & xy & yz & zx & x & y & z & 1 \end{bmatrix}^T
\end{aligned}
\tag{1}
$$

When general quadric surfaces except particular shapes such as imaginary surfaces, planes or straight lines are written in the standard form, they are classified as shown in Table 1. When the surface shape of general earthenware is considered, it is available to approximate it by cone, ellipsoid, one-sheet hyperboloid, two-sheet hyperboloid, hyperbolic paraboloid and elliptic cylinder.

Table 1. Standard forms of quadric surfaces

Name	Standard form
Cone	$ax^2 + by^2 - cz^2 = 0$
Ellipsoid	$ax^2 + by^2 + cz^2 = 1$
One-sheet hyperboloid	$ax^2 + by^2 - cz^2 = 1$
Two-sheet hyperboloid	$ax^2 - by^2 - cz^2 = 1$
Elliptic paraboloid	$ax^2 + by^2 = z$
Hyperbolic paraboloid	$ax^2 - by^2 = z$
Elliptic cylinder	$ax^2 + by^2 = 1$
Hyperbolic cylinder	$ax^2 - by^2 = 1$
Parabolic cylinder	$ax^2 = z$

Quadric surfaces can be parametrically expressed by using two angle parameters for the coordinate of a point on a curved surface. The parametric expression varies depending on the classification of quadric surfaces. Equations (2) and (3) show parametric expressions of quadric surfaces.

Ellipsoid:

$$\begin{aligned} x &= A\cos\theta\sin\phi & 0 \le \theta \le 2\pi \\ y &= B\sin\theta\sin\phi & 0 \le \phi \le 2\pi \\ z &= C\sin\phi \end{aligned} \qquad (2)$$

One-sheet hyperboloid:

$$\begin{aligned} x &= A\cos\theta\cosh\phi & 0 \le \theta \le 2\pi \\ y &= B\sin\theta\sinh\phi & -\pi \le \phi \le \pi \\ z &= C\sinh\phi \end{aligned} \qquad (3)$$

2.5 Principal-axis transformation

This section describes principal-axis transformation, by which general form of quadric surfaces shown in Equation (1) is transformed to the standard form in order to classify quadric surfaces described in section 2.4. Equation (1) is transformed to an algebra-style equation (4) by using the following matrix α, β:

$$\begin{aligned} F = {} & a_{11}x^2 + a_{22}y^2 + a_{33}z^2 \\ & + 2a_{12}xy + 2a_{23}yz + 2a_{13}zx \\ & + 2b_1x + 2b_2y + 2b_3z + d \end{aligned}$$

$$\alpha = \begin{bmatrix} a_{11} & a_{12} & a_{13} \\ a_{21} & a_{22} & a_{23} \\ a_{31} & a_{32} & a_{33} \end{bmatrix}, a_{ij} = a_{ji}, \beta = \begin{bmatrix} b_1 \\ b_2 \\ b_3 \end{bmatrix}, X = \begin{bmatrix} x \\ y \\ z \end{bmatrix}$$

$$F = X^T \alpha X + 2\beta^T + d = 0 \qquad (4)$$

Since matrix α is defined as a real symmetric matrix, using orthogonal matrix P enables diagonalization like Equation (5). An orthogonal base is used in the Lagrange multiplier method as well as the principal-axis transformation. In this paper, an orthogonal base is calculated by using the Gram-Schmidt orthogonalization.

$$P^T \alpha P = P^{-1} \alpha P = \begin{bmatrix} \lambda_1 & 0 & 0 \\ 0 & \lambda_2 & 0 \\ 0 & 0 & \lambda_3 \end{bmatrix} \qquad (5)$$

where $\lambda_1, \lambda_2, \lambda_3$ are eigenvalues of matrix α.

When the solution of $\alpha X + \beta = 0$ is X, X is a vector that moves on a quadric surface and P is a matrix that rotates on a quadric surface.

If the rank of matrix α is 3, quadric surfaces are central quadrics. If the rank is 1 or 2, quadric surfaces are non-central quadrics. If the center exists, the quadric surface should be rotated after it is moved. If the center does not exist, the quadric surface should be moved after it is rotated. This enables transformation of Equation (1) to the standard form. Table 2 shows the classification of quadric surfaces and their ranks.

Table 2. Quadric surfaces and their ranks

Name	Rank
Cone	3
Ellipsoid	3
One-sheet hyperboloid	3
Two-sheet hyperboloid	3
Elliptic paraboloid	2
Hyperbolic paraboloid	2
Elliptic cylinder	2
Hyperbolic cylinder	2
Parabolic cylinder	1

2.6 Local surface fitting with octree

Ohtake presented a method [16] that fits a local area of a point cloud by using an implicit function. An original point cloud is segmented by an octree method. If a surface cannot be obtained within the specified tolerance, the cell is subdivided sequentially. Since surface fitting is performed locally from the point set within the cell, the whole shape can be represented by blending of local surfaces. Therefore, it is unclear whether a principal axis can be derived, so that the whole surface shape does not consider a surface of revolution. In addition, their method requires the normal vector for each point. Therefore, it is necessary to estimate the normal vector on all points. This means that the calculation cost increases. As the result, their method cannot be applied directly to fit surfaces from the earthenware as rotational shapes.

3. Proposed Method

3.1 Removal of uneven portions on earthenware

The smoothing technique [12] based to the Taubin's method is applied to the polygon model created from the point cloud. To be more efficient, some parameters in the transfer function is changed.

In Fig. 1, the polygon model in the left is created directly from the point cloud, and the polygon model in the right is smoothed by applying the smoothing method for 1,000 times. It is obvious that most of the uneven portions are removed. In the following description, polygon and point clouds indicate those after smoothing, unless otherwise specifically noted.

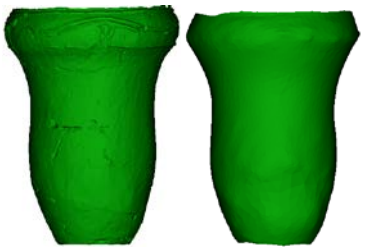

Fig.1 Polygon created from point data and smoothed polygon

3.2 Quadric surface fitting

We paid attention to the fact that earthenware surfaces are close to the rotational shapes. If they are rotational shapes, their cross sections cut by a plane orthogonal to the principal axis will be ellipses. A

quadric surface is well-known as a shape whose cross section is elliptic. If a part of a quadric surface can be determined, its rotational shape can be defined. This means that, even if some portions of a point cloud are missing, they can be interpolated easily from the rest of the point cloud. With these reasons, for estimation of the surface shape of earthenware, quadric surface fitting is appropriate and the technique is examined. General approach of the quadric surface fitting is to apply the least squares method to the Euclidean distance between the point cloud and the quadric surface. In the least squares method that minimizes the Euclidean distance between the point cloud and the quadric surface, the evaluation function is non-linear. Therefore, to obtain a solution, it is necessary to use the Levenberg-Marquardt law or the Newton's method. In these methods, the initial values are important factors. It is difficult, however, to set such initial values of quadric surfaces from earthenware whose manufacturing precision is low. Therefore, these methods are difficult to apply to estimate the surface shape of earthenware.

To determine the distance between the point and the quadric surface algebraically, the Lagrange multiplier method is effective. In order to apply the method to earthenware, it is necessary to consider hyperboloids, paraboloids or elliptic cylindrical surfaces as well as ellipsoids. Therefore, in our method, the extended method by Douros [15] is used for quadric surface fitting. In addition, by adding new constraints, quadric surface fitting is performed using two types of accuracy.

For computing the coefficients of Equation (1), the Lagrange multiplier method is used. The details of the solution are provided in Appendix, *Problem of the Lagrange multiplier method*. In order to solve the Lagrange multiplier method, it is necessary to indicate the constraint expression. This paper uses Equation (6) of the Douros method [15] as the first constraint for Equation (1):

$$u^2 + v^2 + w^2 = 1 \tag{6}$$

Douros et al. applied Equation (6) as a constraint because the solution cannot be obtained within the specified tolerance although the constraint of Equation (8) gives the mathematically optimal solutions. For the same reason, we use this constraint of Equation (6) to generate quadric surfaces. Equation (6) is expressed in the form of Equation (7) using the matrix C:

$$A^T CA = \begin{bmatrix} a & b & c & p & q & r & u & v & w & d \end{bmatrix} C \begin{bmatrix} a \\ b \\ c \\ p \\ q \\ r \\ u \\ v \\ w \\ d \end{bmatrix} = 1 \tag{7}$$

When Equation (7) is set as the constraint, matrix C is calculated as follows:

$$C = \begin{bmatrix} 0 & 0 & 0 & 0 & 0 & 0 & 0 & 0 & 0 & 0 \\ 0 & 0 & 0 & 0 & 0 & 0 & 0 & 0 & 0 & 0 \\ 0 & 0 & 0 & 0 & 0 & 0 & 0 & 0 & 0 & 0 \\ 0 & 0 & 0 & 0 & 0 & 0 & 0 & 0 & 0 & 0 \\ 0 & 0 & 0 & 0 & 0 & 0 & 0 & 0 & 0 & 0 \\ 0 & 0 & 0 & 0 & 0 & 0 & 0 & 0 & 0 & 0 \\ 0 & 0 & 0 & 0 & 0 & 0 & 1 & 0 & 0 & 0 \\ 0 & 0 & 0 & 0 & 0 & 0 & 0 & 1 & 0 & 0 \\ 0 & 0 & 0 & 0 & 0 & 0 & 0 & 0 & 1 & 0 \\ 0 & 0 & 0 & 0 & 0 & 0 & 0 & 0 & 0 & 0 \end{bmatrix}$$

When the Lagrange multiplier method is used, Equation (8) gives the mathematically optimal solution. Therefore, Equation (8) is applied to the second constraint. Douros et al. did not apply this constraint because the solution cannot be obtained within the specified tolerance although the constraint gives the mathematically optimal solutions.

In our method, Equation (8) is introduced to calculate the virtual principal axis. The virtual principal axis is described in the next section. To determine a virtual principal axis, it is necessary to divide a point cloud into groups. Since Equation (8) is introduced as the constraint only for the estimation of the principal axis of the quadric surfaces, it is possible to set a larger tolerance.

$$a^2 + b^2 + c^2 + p^2 + q^2 + r^2 + u^2 + v^2 + w^2 + d^2 = 1 \tag{8}$$

Matrix C is calculated as follows and represented by an expression similar to Equation (7).

$$C = \begin{bmatrix} 1 & 0 & 0 & 0 & 0 & 0 & 0 & 0 & 0 & 0 \\ 0 & 1 & 0 & 0 & 0 & 0 & 0 & 0 & 0 & 0 \\ 0 & 0 & 1 & 0 & 0 & 0 & 0 & 0 & 0 & 0 \\ 0 & 0 & 0 & 1 & 0 & 0 & 0 & 0 & 0 & 0 \\ 0 & 0 & 0 & 0 & 1 & 0 & 0 & 0 & 0 & 0 \\ 0 & 0 & 0 & 0 & 0 & 1 & 0 & 0 & 0 & 0 \\ 0 & 0 & 0 & 0 & 0 & 0 & 1 & 0 & 0 & 0 \\ 0 & 0 & 0 & 0 & 0 & 0 & 0 & 1 & 0 & 0 \\ 0 & 0 & 0 & 0 & 0 & 0 & 0 & 0 & 1 & 0 \\ 0 & 0 & 0 & 0 & 0 & 0 & 0 & 0 & 0 & 1 \end{bmatrix}$$

In this paper, as Equations (6) and (8) are set as constraints and the Lagrange multiplier method is used to solve the general formula of quadric surfaces (1). Using the method described in section 2.4, Equation (1) is transformed to the standard quadric form as shown in Table 1. Then the quadric surfaces are classified as described in section 2.5 to obtain the quadric surface information.

3.3 Determination of principal axis

In our method, a point cloud is divided into groups and an earthenware surface is defined as several pieces of quadric surfaces. When a point cloud is divided, the division along an axis must be determined. The principal axis is suitable if all of the point clouds can

be fitted to one quadric surface. Quadric surfaces contain at least one principal axis without the presence of the surface central axes. This means that, even if a point cloud is fitted to any curved surface, it is possible to specify the principal axis. In addition, even if a quadric surface distant from the point cloud is calculated, the created quadric surface is a rotational shape and therefore its principal axis will not be different so much.

As the constraint for a quadric surface fitting, our method introduces Equation (8) to determine the principal axis that can pass through the principal rotational axis. This is because Equation (6) is insufficient condition to derive the suitable principal axis. Consequently, as the constraint condition for a rough principal axis, both Equations (6) and (8) are verified to be appropriate. Fig. 2 shows the front and back views of the polygon models of Fig. 1, whose principal axes displayed with red lines are obtained using Equations (6) and (8). The principal axis calculated using Equation (6) does not lie at the center of the polygons.

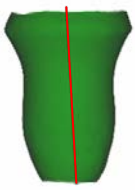

(a) Principal axis (red line) obtained by Equation (6)
(front view)

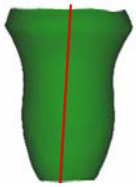

(b) Principal axis (red line) obtained by Equation (6)
(back view)

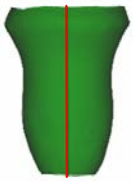

(c) Principal axis (red line) obtained by Equation (8)
(front view)

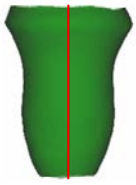

(d) Principal axis (red line) obtained by Equation (8)
(back view)

Fig. 2 Difference of the principal axes depending on constraints

3.4 Division of point cloud for quadric surface fitting

In order to divide the point cloud into several groups, the point cloud is fitted to a quadric surface within the specified tolerance by using the principal axis calculated in section 3.3. First, the interval of division is determined along the principal axis. Next, using the coordinate of the point cloud defined from the interval, a quadric surface is fitted by using the method described in section 3.2. The distance between the quadric surface and the point cloud is evaluated and a quadric surface is defined for each point cloud within the tolerance. In quadric surface fitting described in this section, Equation (6) is used as the constraint. This is because the solution might not be obtained when the Equation (8) is used. Even if the solution is obtained, the number of groups in the point cloud will be large and a large number of quadric surfaces must be defined for earthenware. Therefore, as for the reasonable number of division, Equation (6) is used as the constraint. The overview of the process is described below:

1. Decide the length of the principal axis

   Since the principal axis calculated in section 3.3 is infinite, the principal axis is defined only for the interval where a point cloud exists. All point clouds are projected onto the principal axis and two points that form the maximum distance on the principal axis are obtained. The obtained points are set as the start and end points of the axis. Fig. 3 shows the point cloud and the red line shows the principal axis. For easier view, the density of the point cloud was decreased to 20% of the actual one.

Fig. 3 Point cloud and principal axis

2. Divide the point cloud according to the planes

   Since there are ten coefficients for Equation (1), at least ten points are required for quadric surface fitting. Planes whose normals are the principal axes in step 1 are considered. On the principal axis, it is possible to retrieve point clouds included in a region sandwiched by the two planes. In addition, the point cloud is divided so that each of the divided groups contains ten or more points. For example, if the principal axis is divided into 100 intervals, 100 groups of point clouds are generated. Thus, each group will contain about 50 points in case of the point cloud shown in Fig.1. Accordingly 1/100 of the length of the principal axis is set as the unit of movement. The created quadric surface is evaluated with original point cloud by using maximum and average distance. The length obtained by dividing the principal axis into 100 intervals is set to ***dz*** and the start point of the principal axis is set to ***s*** and the end point is

set to ***e***. Plane 1 is defined as a plane that passes through one of the points ***s*** or ***e*** and contains the normal vector on the principal axis. Plane 2 is defined as a plane translated from plane 1 by distance ***dz***. Point clouds delimited by plane1 and plane 2 are obtained. Fig. 4 shows the point clouds between two planes, where ***dz*** is multiplied several times from the actual utilization values. In Fig.4, the red line is the principal axis shown in Fig.3.

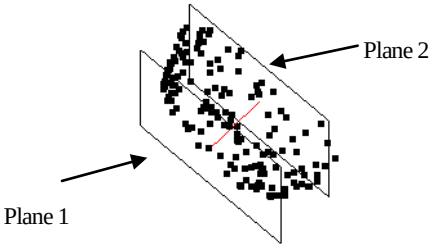

Fig. 4 Point cloud delimited by two planes

3. Quadric surface fitting and evaluation

A quadric surface is fitted to the point cloud sampled in step 2. If quadric surfaces are created from point clouds in a wide range as much as possible, the number of quadric surfaces to be created can be reduced. Accordingly, with the specified tolerance (average distance and maximum distance), the distance between the point clouds and quadric surfaces is evaluated. The average distance between the point cloud and the quadric surface is derived from the average obtained by projecting each point in a region between the two planes. The maximum distance is calculated in the same manner as the average distance. If the distance is equal to or smaller than the tolerance, translate plane 2 by ***dz*** along the axis to increase the intervals delimited by planes 1 and 2. Then, repeat the fitting. If the distance is greater than the tolerance, quadric surfaces will be defined for the point clouds in the previous interval. To be more specific, by plane 2 moved by ***–dz*** along the axis, points are defined in the interval delimited by planes 1 and 2. A quadric surface is fitted to these points, and the quadric surface information is saved. Then, plane 1 is moved to the position of plane 2 and the process of steps 2 and 3 is repeated. As planes 1 and 2 coincide, the processing is terminated. In Fig. 5, the red points are fixed as quadric surface and planes 1 and 2 are redefined and the red line is the principal axis in Fig.3.

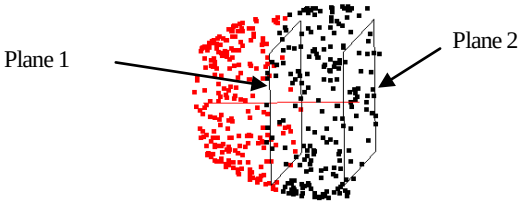

Fig. 5 Point clouds set as a quadric surface and definition of new planes

Fig. 6 visualizes quadric surfaces generated from the axes of principal and point cloud groups. These are parts of quadric surfaces, generated only for the portions where point clouds exist. The initial tolerance is 0.5mm for the average distance and 1.0mm for the maximum distance. If surface fitting fails, the tolerance will be set to a greater value, from 50 to 100% of the initial one for the next fitting. For generating the surfaces in Fig. 6, the following tolerance is set: 1mm or smaller for the average distance and 4mm or smaller for the maximum distance. Along the virtual principal axis, quadric surfaces are fitted to the point clouds in order. The fixed point clouds are excluded for the subsequent application. In other words, whenever a group of the point cloud is fixed as a quadric surface, the number of the points available will continue to decline. In our method, the ellipsoid shown in Fig. 6 (d) is fitted after the quadric surfaces of (a), (b) and (c) are fixed. Due to this, point clouds cannot be chosen so flexibly and quadric surfaces cannot be fitted with using the same tolerance. Therefore, quadric surfaces are fitted by using the default initial tolerance. For the intervals for which the surfaces cannot be fitted, the tolerance is loosened to 1.5mm for the average distance and 6mm for the maximum distance. Fig. 6 (e) shows the all the surfaces of (a), (b), (c) and (d) drawn at the same time.

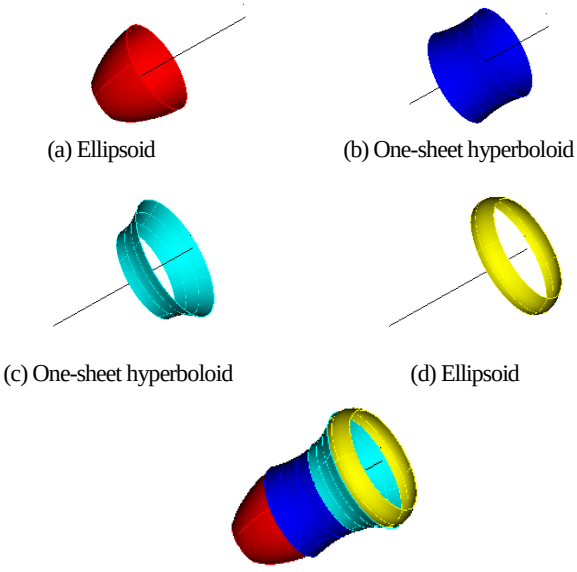

(a) Ellipsoid (b) One-sheet hyperboloid

(c) One-sheet hyperboloid (d) Ellipsoid

(e) All groups

Fig.6 Quadric surfaces for point cloud groups

3.5 Free-form surface generation from quadric surfaces

Earthenware surfaces can be represented with two or more quadric surfaces by using the method described in section 3.4. If earthenware surfaces can be represented with quadric surfaces, the method can be used for a wide range of applications. Examples are as follows:

1. There are so many missing parts in earthenware that they cannot be interpolated from the peripheral information.

2. The surface is set as the reference for optimizing the location of earthenware pieces.

In this paper, we propose a method to reproduce free-form surfaces from quadric surfaces. For the reproduction processing, missing portions between separate quadric surfaces must be interpolated. In our method, the tolerance is set to guarantee the distance equal to or smaller than 1mm on an average (1.5 mm for some portions). Thus, sample points are generated on quadric surfaces for interpolating missing portions and a free-form curve mesh is generated from the sample points. A region enclosed by the generated four free-form curves is interpolated by a surface with good accuracy for earthenware. In addition, by using the four free-form curves, it is not necessary to generate trimmed surfaces, which will make operation easier for the created free-form surfaces. The overview of the processing is described below:

1. Generate sample points on each quadric surface

   Each quadric surface has its principal axis. The axis is divided equally to the specified number of intervals and a plane whose normal is the principal axis is defined to pass through one of the division points. Sample points are generated on the intersection curve between the quadric surface and the defined plane. According to the classification described in section 2.5, each point is represented parametrically. By setting the number of division for the principal axis and that for intersection (ellipse), the coordinates of the sample points can be easily calculated. Fig. 7 shows the sample points generated on quadric surfaces.

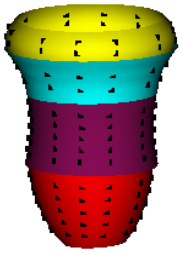

Fig. 7 Sample points on quadric surfaces

2. Generate a curve mesh

   The sample points are interpolated in each of ***u*** and ***v*** directions. The ***u*** direction here indicates the direction of principal of each quadric surface and the ***v*** direction indicates the direction of the principal axis. By generating a Bezier curve that passes through a point [17], one Bezier curve is always generated between vertices. In this paper, a free-form curve passing through the point is generated, while at each point, the normal vector and the tangent vectors in the ***u*** and ***v*** directions can be obtained. It is also possible to generate a free-form curve with high accuracy using the points, normals and tangent vectors, which are introduced in the document [17]. Fig. 8 is an example where sample points are interpolated with Bezier curves.

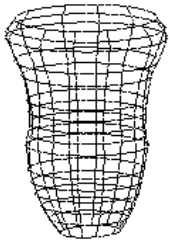

Fig. 8 Generated curve mesh

3. Interpolate a curve mesh

   Since Bezier curves always pass through sample points, every end point of Bezier curves coincides with any of the end points of Bezier curves. Due to this, it is easy to generate a surface to a region enclosed with four sides. In this paper, a Gregory surface [18] is generated since it is easy to generate the surface from four Bezier curves. Fig. 9 shows Gregory surfaces generated to regions enclosed with four Bezier curves.

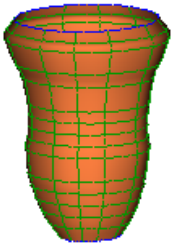

Fig. 9 Result of surface interpolation

4. Experimental Result

This section describes the results of applying our method to earthenware pieces. The earthenware pieces used in the experiment are borrowed from Iseki No Manabi-kan at Morioka City. We used a PC with the CPU of Intel Core2 Duo 2.80GHz and 3.48GB memory in the experiments.

Fig. 10 shows a polygon model obtained by smoothing polygons, whose location and posture are determined three-dimensionally from measured point clouds by using the method described in section 3.1. The number of polygons is 11,726. The experiment is carried out for the model shown in Fig. 10. The bounding box size of the model in Fig. 10 is 205.6mm (width) x 288.1mm (height) x 208.1mm (depth).

Fig. 10 Smoothed polygon data

First, quadric surfaces generated using the method described in section 3.4 are evaluated whether they are reasonable. Fig. 11 shows the polygons smoothed using the method described in section 3.1 overlapped on quadric surfaces. The portions currently shown in yellow, cyan, blue, and red are fitted to quadric surfaces. A green part shows a polygon model obtained by smoothing polygons, whose location and posture are determined three-dimensionally from the measured point clouds. In the subsequent figures, the same rule of the colors is applied. Table 3 shows the average distances and the maximum distances between the quadric surfaces in Fig. 6 and the vertices on the smoothed polygons. The quadric surfaces are generated with the tolerance equal to or smaller than 1mm for the average distance (1.5mm for some portions), while the distances for some portions are the ones shown in Table 3. As the measured maximum distances are compared to 205.6mm, the minimum side of the boundary box of the model, the gap is about 1.9% (2.6% for some portions). This quality is judged to be sufficient for restoration of earthenware. But the proposed method removes uneven portions on surfaces by applying the smoothing technique. If the whole shape is distorted by the removal, it is difficult to apply this method.

Fig. 11 Comparison of quadric surfaces and polygons

Table 3. Maximum distances between sample points and quadric surfaces

Quadric surface	Average distance	Maximum distance
(a) Ellipsoid	0.57mm	3.82mm
(b) One-sheet hyperboloid	0.62mm	3.93mm
(c) One-sheet hyperboloid	0.51mm	3.33mm
(d) Ellipsoid	1.06mm	5.40mm

Then, the generated free-form surfaces are evaluated whether they represent the whole shape properly. Fig. 12 shows the smoothed polygons overlapped on the generated free-form surfaces. The portions shown in orange are free-form surfaces generated by using the method described in section 3.5. It is possible to find that they are almost coincident. The average separation distance is 1.31mm and the maximum separation distance is 6.01mm.

Fig. 12 Earthenware pieces and polygon data smoothed with the Taubin's method

Fig. 13 shows the data from which some polygons of the model in Fig. 10 are removed randomly. The bounding box size of the model in Fig. 13 is 205.6mm (width) x 288.1mm (height) x 208.1mm (depth). The number of polygons is 6,546.

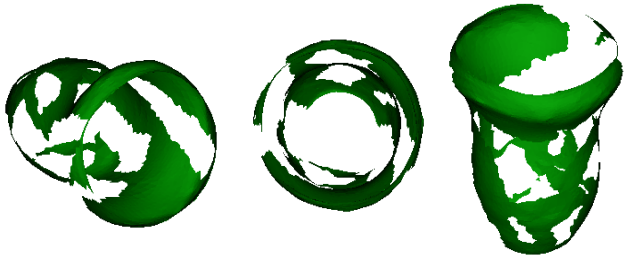

Fig. 13 Polygon model some of whose point clouds are removed

First, quadric surfaces fitted to the data of Fig. 13 and the data of Fig. 6 are compared. Fig.14 shows two kind of quadric surfaces. One is from complete polygons shown in Fig.6 and the other is from incomplete polygons shown in Fig.13. The quadric surfaces generated from the polygons in Fig. 13 are shown in magenta. Both surfaces are almost coincident. This means that the number of point clouds does not affect quadric surface fitting. In addition, since the length along the principal axis is not changed greatly, the number of point clouds does not affect grouping of point clouds.

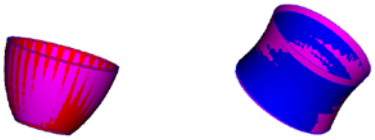

(a) Ellipsoid (b) One-sheet hyperboloid

(c) One-sheet hyperboloid (d) Ellipsoid

Fig. 14 Overlap of quadric surfaces

In the end, Fig. 15 shows the free-form surface data generated from the polygon data in Fig. 13 overlapped on those generated from the polygon data in Fig. 10. The free-form surfaces shown in magenta are generated from the data of Fig. 13 and those in orange are the ones shown in Fig. 12. It is possible to find that the surfaces are almost coincident.

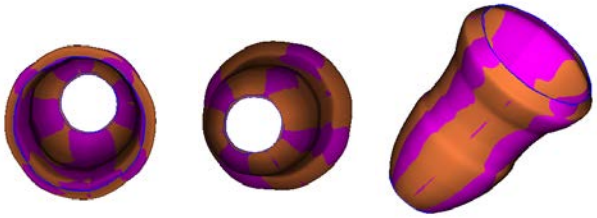

Fig. 15 Overlap of free-form surfaces

To confirm the efficacy against other earthenware, our method is applied to other earthenware. In Fig. 16 (a), the polygon model is created directly from the point cloud of earthenware without missing portions. The number of polygons is 194,639. The bounding box size of the model is 124.4mm (width) x 183.3mm (height) x 142.4mm (depth). The smoothed polygon model is generated by applying the Taubin's method as shown in Fig.16 (b). For the polygon model in Fig. 1, most of the uneven portions could be removed by applying the smoothing method for 1,000 times, but the polygon model in Fig. 16 is smoothed by applying the smoothing method for 10,000 times because the height difference at uneven portions is large. Then, the initial value of the number of application times is set to 1,000 and the test is repeated for 2,000 times, 3,000 times and more in increments of 1,000. As a result, the number of application times is set to 10,000, in which most of the patterns on surfaces are removed.

(a) Polygon created from point data

(b) Polygon smoothed by applying the Taubin's method for 10,000 times

Fig. 16 Excavated earthenware 1

Fig. 17 shows the results of the quadric surface estimation by the proposed method. The point clouds were divided into four segments. For generating the surfaces in Fig. 17, the following tolerance is set: 1.5mm or smaller for the average distance and 8.0mm or smaller for the maximum distance. The tolerance is set by the same method as the one described in section 3.4. Fig.18 shows the polygons of Fig. 16 (b) overlapped on quadric surfaces. The green portions show the polygon models obtained by smoothing polygons, whose location and posture are determined three-dimensionally from the measured point clouds. Table 4 shows the average distances and the maximum distances between the quadric surfaces in Fig. 17 and the vertices on the smoothed polygons. The ellipsoid shown in Fig. 17 (b) has the longest distance. As the measured maximum distances are compared to 124.4mm, the minimum side of the bounding box of the model, the gap is about 6.2%. This quality is judged to be sufficient for restoration of earthenware.

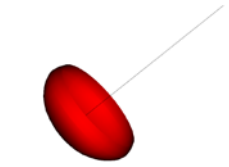

(a) Ellipsoid

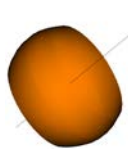

(b) Ellipsoid

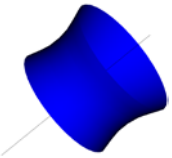

(c) One-sheet hyperboloid

(d) One-sheet hyperboloid

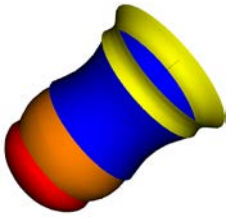

(e) All groups

Fig.17 Quadric surfaces for point cloud groups

Fig.18 Comparison of quadric surfaces and polygons

Table 4. Maximum distances between sample points and quadric surfaces

Quadric surface	Average distance	Maximum distance
(a) Ellipsoid	1.27mm	5.39mm
(b) Ellipsoid	1.12mm	7.69mm
(c) One-sheet hyperboloid	0.82mm	3.58mm
(d) One-sheet hyperboloid	0.84mm	4.38mm

Next, to confirm the efficacy against earthenware with missing portions, our method is applied to assembled earthenware excavated from ruins. Fig. 19 (a) shows assembled earthenware excavated from ruins, where more than half of earthenware is missing. The number of polygons is 117,257. The bounding box size of the model is 154.1mm (width) x 213.2mm (height) x 141.3mm (depth). Fig. 19 (b) shows polygon models obtained by smoothing polygons using the Taubin's method.

(a) Polygon created from point data

(b) Polygon smoothed by applying the Taubin's method for 1,000 times

Fig. 19 Excavated earthenware 2

Fig. 20 shows a quadric surface generated from the principal axis and point clouds. For generating the surface in Fig. 20, the following tolerance is set: 1.0mm or smaller for the average distance and 6.5mm or smaller for the maximum distance. The tolerance is set by the same method as the one described in section 3.4. Fig.21 shows the polygons of Fig. 19 (b) overlapped on the quadric surface. The green portions show polygon models obtained by smoothing polygons, whose location and posture are determined three-dimensionally from the measured point clouds. Table 5 shows the average distances and the maximum distances between the quadric surfaces in Fig. 19 and the vertices on the smoothed polygons. As the measured maximum distances are compared to 141.3mm, the minimum side of the bounding box of the model, the gap is about 4.4%. This quality is judged to be sufficient for restoration of earthenware. It shows the effectiveness for damaged earthenware.

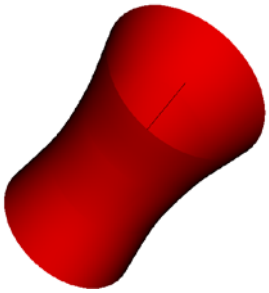

(One-sheet hyperboloid)

Fig.20 Quadric surface for point cloud groups

Fig.21 Comparison of quadric surfaces and polygons

Table 5. Maximum distance between sample points and quadric surfaces

Quadric surface	Average distance	Maximum distance
Ellipsoid	0.74mm	6.17mm

5. Conclusion and Future Issue

In this paper, we proposed the method of fitting quadric surfaces created by the point clouds to earthenware. In our method, the Taubin's smoothing method is applied to measured point clouds and the portions with uneven patterns are removed. After that, quadric surfaces are fitted to all point clouds and the principal axis is determined for dividing the point clouds into groups. By repeating the division of point clouds along the principal axis and fitting quadric surfaces to the point clouds, the point clouds are divided most appropriately for quadric surface fitting. Earthenware surfaces can be expressed with the generated quadric surfaces. In addition, by using points on quadric surfaces, the method to represent the entire surface of earthenware with free-form surfaces is described. In the future, the method is extended for thickening shapes or optimizing the posture of earthenware pieces.

Part of this work was supported by JSPS KAKENHI Grant Number 2050088.

The basic concept of our method has already been presented in NICOGRAPH International 2013[19] and this paper is the extended one. We are extremely grateful for efficient advice from the paper reviewers.

Appendix

As the point is set as X, consider the problem of fitting a quadric surface to a set of points. Equation (a-1) is a quadric form representing a quadric surface.

$$\begin{aligned} &F(X,A) = AX = \\ &ax^2 + by^2 + cz^2 + pxy + qyz + rzx + ux + vy + wz + d = 0 \\ &A = \begin{bmatrix} a & b & c & p & q & r & u & v & w & d \end{bmatrix}^T \\ &X = \begin{bmatrix} x^2 & y^2 & z^2 & xy & yz & zx & x & y & z & 1 \end{bmatrix}^T \end{aligned} \tag{a-1}$$

For an arbitrary point (x_i, y_i, z_i), X_i is defined as follows:

$$X_i = \begin{bmatrix} x_i^2 & y_i^2 & z_i^2 & x_i y_i & y_i z_i & z_i x_i & x_i & y_i & z_i & 1 \end{bmatrix}^T$$

If point (x_i, y_i, z_i) lies on the quadric surface, $F(X_i, A) = 0$ is obtained, otherwise, $F(X_i, A)^2 > 0$ is obtained.

In other words, by determining A that minimizes Equation (a-2) below, Equation (a-1) for the quadric surface can be defined.

$$\sum \left\{ F(Xi, a)^2 \mid i = 1,2,\cdots n \right\} \tag{a-2}$$

This is redefined as a problem of matrix.

$$D = \begin{bmatrix} x_1^2 & y_1^2 & z_1^2 & x_1y_1 & y_1z_1 & z_1x_1 & x_1 & y_1 & z_1 & 1 \\ x_2^2 & y_2^2 & z_2^2 & x_2y_2 & y_2z_2 & z_2x_2 & x_2 & y_2 & z_2 & 1 \\ \vdots & \vdots & \vdots & \vdots & \vdots & \vdots & \vdots & \vdots & \vdots & \vdots \\ x^2{}_n & y_n^2 & z_n^2 & x_ny_n & y_nz_n & z_nx_n & x_n & y_n & z_n & 1 \end{bmatrix}$$

If the matrix D defined with a row of X_i at all vertices is defined as shown above, this will be the problem to minimize

$$\|DA\|^2 = A^T D^T DA \tag{a-3}$$

In addition, when Equation (a-3) is minimized, this problem can be replaced with the one solving the Lagrange multiplier method by adding the constraint to A. Fitzgibbon et al. sets Equation (a-4) as the condition for defining Equation (a-1) to be an ellipse.

$$\begin{aligned} &F(X,A) = AX = \\ &ax^2 + by^2 + pxy + ux + vy + d = 0 \\ &A = \begin{bmatrix} a & b & p & u & v & d \end{bmatrix}^T \end{aligned} \tag{a-4}$$

$$X = \begin{bmatrix} x^2 & y^2 & xy & x & y & 1 \end{bmatrix}^T$$

In addition, the constraint condition is set by Equation (a-5).

$$p^2 - 4ab = -1 \tag{a-5}$$

In this paper, it is necessary to handle general quadric surfaces including ellipsoids and different constraints must be set.

Douros describes the constraints that they use. The constraint is set as the partial differential vector at the origin is set to the unit vector. If a differential vector is defined as

$$\nabla F = \begin{bmatrix} 2ax + py + rz + u \\ 2by + px + qz + v \\ 2cz + qy + rx + w \end{bmatrix}$$

$\nabla F|_{x=y=z=0} = \begin{bmatrix} u \\ v \\ w \end{bmatrix}$ is obtained, which means

$$u^2 + v^2 + w^2 = 1 \tag{a-6}$$

If Equation (a-6) is rewritten using a matrix, the following is obtained.

If

$$C = \begin{bmatrix} 0 & 0 & 0 & 0 & 0 & 0 & 0 & 0 & 0 & 0 \\ 0 & 0 & 0 & 0 & 0 & 0 & 0 & 0 & 0 & 0 \\ 0 & 0 & 0 & 0 & 0 & 0 & 0 & 0 & 0 & 0 \\ 0 & 0 & 0 & 0 & 0 & 0 & 0 & 0 & 0 & 0 \\ 0 & 0 & 0 & 0 & 0 & 0 & 0 & 0 & 0 & 0 \\ 0 & 0 & 0 & 0 & 0 & 0 & 0 & 0 & 0 & 0 \\ 0 & 0 & 0 & 0 & 0 & 0 & 1 & 0 & 0 & 0 \\ 0 & 0 & 0 & 0 & 0 & 0 & 0 & 1 & 0 & 0 \\ 0 & 0 & 0 & 0 & 0 & 0 & 0 & 0 & 1 & 0 \\ 0 & 0 & 0 & 0 & 0 & 0 & 0 & 0 & 0 & 0 \end{bmatrix}$$

then

$$A^T CA = \begin{bmatrix} a & b & c & p & q & r & u & v & w & d \end{bmatrix} C \begin{bmatrix} a \\ b \\ c \\ p \\ q \\ r \\ u \\ v \\ w \\ d \end{bmatrix} = 1 \tag{a-7}$$

To summarize the above, the quadric surface fitting problem becomes the problem of the general Lagrange multiplier method shown below, where Equation (a-3) is minimized under the constraints of Equation (a-7).

[Problem of the Lagrange multiplier method]

A is obtained to minimize the following:

$L(A,\lambda) = A^T D^T DA - \lambda(A^T CA - 1)\ \lambda > 0$

References

[1] M.Sakamoto, S.Yasuhara, M.Kanou, S.Kato, H.Itoh, A Contour Mating Method using Hierarchical Contour Expression and its Application on Earthenware Reconstruction, Imaging & Visual Computing The Journal of the Institute of Image Electronics Engineers of Japan, Vol.34, No.3 , pp.228-235, 2005.

[2] QiXing Huang, S.Flory, N.Gelfand, M.Hofer and H.Pottmann, Reassembling Fractured Objects by Geometric Matching, ACM SIGGRAPH 2006, pp.569-578, 2006.

[3] B.Brown, C.Toler-Franklin, D.Nehab, M.Burns, A.Vlachopoulos, C.Doumas, D.Dobkin, S.Rusinkiew- icz and T.Weyrich, A System for High-Volume Acquisition and Matching of Fresco Fragments: Reassembling Theran Wall Paintings, ACM Transactions on Graphics (Proc. SIGGRAPH) 2008, Vol.27, No.3, 2008.

[4] K. Shoji, K. Konno, T. Konno, F. Chiba, An Algorithm of Fracture Matching Based on Measured Point Set of Fragment Surface, IWAIT 2011, CD-ROM, 2011.

[5] E. Altantsetseg, Y. Muraki, F. Chiba, and K. Konno, 3D Surface Reconstruction of Stone Tools by Using Four-Directional Measurement Machine, The International Journal of Virtual Reality (IJVR), Vol.10, No.1, pp.37-43, 2011.

[6] K.Hori, M.Imai, T.Ogasawara, Data Model for Computer Reconstruction of Potsherds,Japan Society for Archaeological Information, Vol.5, No.2, pp.1-10, 1999.

[7] K.HoriI, M.Imai, T.Ogasawara, Hierarchical Description of a Contour for Reconstruction of Broken Earthenware, IEICE Trans, D-II, Vol.J83-D-II, Vol.5, pp.1329-1394, 2000.

[8] M.Kano, S.Kato, H.Itoh, A Fast Joint Detection Method Based on Difficulty of Discrimination, Transactions of Information Processing Society of Japan, Vol.42, No. 11, pp.2689-2698, 2001.

[9] S. Oikawa, C.Li, K.Matsuyama, K.Konno, Y.Tokuyama, An Examination of Matching Algorithm Considering Pattern Flow of Cord-Wrapped Stick Pattern for Earthenware Restoration, IWAIT2013, pp.366-371, CD-ROM, 2013.

[10] K.Konno, N.Abe, F.Chiba, Y.Tokuyama, A Study on Generating Section Lines to Make Measured Drawings of Earthenware Artifacts, The journal of the Institute of Image Information and Television Engineers, Vol.61, No.10, pp.1504-1511, 2007.

[11] T.Konno, K.Konno, Column form extraction and shaft estimation using point cloud by 3D measurement: trial reconstruction of the south gate, outer fence of Shiwajo, Japan Society for Archaeological Information, Vol.13, No.2, pp.1-9, 2008.

[12] T.Kinoshita, Y.Muraki, K.Matsuyama, K.Konno, Piece Modeling Method around an Hole to Reconstruct an Earthenware Vessel, The Journal of the Society for Art and Science, Vol.11, No.3, pp.47-58, 2012.

[13] G.Taubin, A signal processing approach to fair surface design, In ACM SIGGRAPH Conference Proceedings, pp.351-358, 1995.

[14] A. Fitzgibbon, M. Pilu, and R.B. Fisher, Direct least square fitting of ellipses, IEEE trans. Pattern Analysis and Machine Intelligence, Vol. 21, No. 5, pp. 476–480, 1999.

[15] I.Douros, B.Buxton, Three-Dimensional Surface Curvature Estimation using Quadric Surface Patches, Scanning 2002 Proceedings, 2002.

[16] Y.Ohtake, A.Belyaev, M.Alexa, Greg Turk, H.Seidel, Multi-level partition of unity implicits, ACM Transactions on Graphics, Vol.22, No. 3, pp. 463-470, 2003.

[17] H.Chiyokura, Solid modeling with DESIGNBASE: theory and implementation, Addison-Wesley Longman Publishing Co., Inc, 1988.

[18] H.Chiyokura, F.Kimura, Design of solids with free-form surface, Computer Graphics, Vol.17, pp.289-298, 1983.

[19] T.Kinoshita, K.Matsuyama, K.Konno, An Estimation of Earthenware's Surface Shape Using Quadric Surfaces, NICOGRAPH International 2013 (12th), 2013.

Tsutomu Kinoshita

Tsutomu Kinoshita is a member of Lattice Technology Co., Ltd. He received a BS in mathematics in 1993 from Science University of Tokyo. He received a Dr. Eng in computer science from Iwate University in 2013. His research interests include geometric modeling and computer graphics. He is a member of the Society for Art and Science.

Katsutsugu Matsuyama

Katsutsugu Matsuyama is currently an assistant professor at Iwate University. His research interests include computer graphics, information visualization and interactive systems. He received BE, ME, DE degrees in computer science from Iwate University in 1999, 2001 and 2005, respectively. He was a research associate at Future University-Hakodate from 2005 to 2011.

Kouichi Konno

Kouichi Konno is a professor of Faculty of Engineering at Iwate University. He received a BS in information science in 1985 from the University of Tsukuba. He earned his Dr. Eng. in precision machinery engineering from the University of Tokyo in 1996. He joined the solid modeling project at RICOH from 1985 to 1999 and the XVL project at Lattice Technology Co., Ltd. in 2000. He worked on an associate professor of Faculty of Engineering at Iwate University from 2001 to 2009. His research interests include virtual reality, geometric modeling, 3D measurement systems, and computer graphics. He is a member of IEEE CS.